

Relic Density of Neutralino Dark Matter in Supergravity Models

V. Barger and Chung Kao

Department of Physics, University of Wisconsin, Madison, WI 53706

Abstract

We calculate the relic density ($\Omega_{\chi_1^0} h^2$) of neutralino dark matter in supergravity models with radiative electroweak symmetry breaking, for values of the Higgs sector parameter $\tan\beta \equiv v_2/v_1$ between the two infrared fixed points of the top quark Yukawa coupling, $\tan\beta \simeq 1.8$ and $\tan\beta \simeq 56$. For $\tan\beta \lesssim 10$, the CP-odd Higgs pseudoscalar (A^0) and the heavier CP-even Higgs scalar (H^0) are much heavier than the lightest neutralino (χ_1^0), and the annihilation cross section of χ_1^0 pairs is significantly enhanced only in the vicinity of the lighter CP-even Higgs boson (h^0) and the Z boson poles. For $\tan\beta \gtrsim 40$, m_A and m_H become comparable to $2m_{\chi_1^0}$, and the neutralino annihilation cross section can be significantly enhanced by the poles of the H^0 and the A^0 as well. For a cosmologically interesting relic density, $0.1 \lesssim \Omega_{\chi_1^0} h^2 \lesssim 0.5$, we find that the supergravity parameter space is tightly constrained. The mass spectra for supersymmetric particles are presented for unification mass parameters in the cosmologically interesting region.

I. INTRODUCTION

A supersymmetry (SUSY) between fermions and bosons provides a natural explanation of the Higgs electroweak symmetry breaking (EWSB) mechanism in the framework of a grand unified theory (GUT). The evolution of renormalization group equations (RGEs) [1] with the particle content of the minimal supersymmetric standard model (MSSM) [2,3] is consistent with a grand unified scale at $M_{\text{GUT}} \sim 2 \times 10^{16}$ GeV and an effective SUSY mass scale in the range $M_Z < M_{\text{SUSY}} \lesssim 1$ TeV. With a large top quark Yukawa coupling to a Higgs boson at the GUT scale, needed for $b-\tau$ Yukawa unification [4,5], radiative corrections can drive the corresponding Higgs boson mass squared parameter negative, spontaneously breaking the electroweak symmetry and naturally explaining the origin of the electroweak scale. In the minimal supersymmetric GUT with a large top quark Yukawa coupling (Y_t), there is an infrared fixed point (IRFP) [5–8] at low $\tan\beta$, and the top quark mass is correspondingly predicted to be $m_t = 200 \text{ GeV} \sin\beta$ [5]. At high $\tan\beta$, another quasi-IRFP solution ($dY_t/dt \simeq 0$) exists at $\tan\beta \sim 60$ [5,7]. For $m_t = 175 \text{ GeV}$, the two IRFPs of top quark Yukawa coupling appear at $\tan\beta \simeq 1.8$ and $\tan\beta \simeq 56$ [5].

Supersymmetry extends the Poincaré symmetry to new dimensions of space and time and local gauge invariance with SUSY includes gravity. In supergravity (SUGRA) models [9], it is assumed that supersymmetry is broken in a hidden sector with SUSY breaking communicated to the observable sector through gravitational interactions, leading naturally but not necessarily [10] to a common scalar mass (m_0), a common gaugino mass ($m_{1/2}$), a common trilinear coupling (A_0) and a common bilinear coupling (B_0) at the GUT scale. Through minimization of the Higgs potential, the B parameter and magnitude of the superpotential Higgs mixing parameter μ are related to the ratio of vacuum expectation values (VEVs) of Higgs fields ($\tan\beta \equiv v_2/v_1$), and the mass of the Z boson (M_Z). The SUSY particle masses and couplings at the weak scale can be predicted by the evolution of RGEs from the unification scale [5,11].

In our analysis, we evaluate SUSY mass spectra and couplings in the minimal supergravity model with four parameters: m_0 , $m_{1/2}$, A_0 and $\tan\beta$; and the sign of the Higgs mixing parameter μ . The neutralino relic density is only slightly affected by a change in the A_0 parameter since A_0 mainly affects the masses of third generation sfermions. Therefore, for simplicity we take $A_0 = 0$ in most of our calculations.

The mass matrix of the neutralinos in the weak eigenstates (\tilde{B} , \tilde{W}_3 , \tilde{H}_1 , \tilde{H}_2) has the following form [5]

$$M_N = \begin{pmatrix} M_1 & 0 & -M_Z \cos\beta \sin\theta_W & M_Z \sin\beta \sin\theta_W \\ 0 & M_2 & M_Z \cos\beta \cos\theta_W & -M_Z \sin\beta \cos\theta_W \\ -M_Z \cos\beta \sin\theta_W & M_Z \cos\beta \cos\theta_W & 0 & \mu \\ M_Z \sin\beta \sin\theta_W & -M_Z \sin\beta \cos\theta_W & \mu & 0 \end{pmatrix}. \quad (1)$$

This matrix is symmetric and can be diagonalized by a single matrix to obtain the mass eigenvalues and eigenvectors. The form of Eq. (1) establishes our sign convention for μ .

Recent measurements of the $b \rightarrow s\gamma$ decay rate by the CLEO [12] and LEP collaborations [13] place constraints on the parameter space of the minimal supergravity model [14]. It was found that $b \rightarrow s\gamma$ excludes most of the minimal supergravity (mSUGRA) parameter space

when $\tan\beta$ is large and $\mu > 0$ [14]. In this article, we present results for both $\mu > 0$ and $\mu < 0$.

We calculate the masses and couplings in the Higgs sector with one loop corrections from both the top and the bottom Yukawa interactions in the RGE-improved one-loop effective potential [15] at the scale $Q = \sqrt{m_{\tilde{t}_L} m_{\tilde{t}_R}}$. With this scale choice, the numerical value of the CP-odd Higgs boson mass (m_A) at large $\tan\beta$ [16] is relatively insensitive to the exact scale and the loop corrections to M_A are small compared to the tree level contribution. In addition, when this high scale is used, the RGE improved one-loop corrections approximately reproduce the dominant two loop perturbative calculation of the mass of the lighter CP-even Higgs scalar (m_h). Our numerical values of m_h are very close to the results of Ref. [17] where somewhat different scales higher than M_Z have been adopted in evaluating the effective potential.

The matter density of the Universe ρ is described in terms of a relative density $\Omega = \rho/\rho_c$ with $\rho_c = 3H_0^2/8\pi G_N \simeq 1.88 \times 10^{-29} h^2 \text{ g/cm}^3$ the critical density to close the Universe. Here, H_0 is the Hubble constant, $h = H_0/(100 \text{ km sec}^{-1} \text{ Mpc}^{-1})$, and G_N is Newton's gravitational constant.

There is compelling evidence from astronomical observations for the existence of dark matter [18]. Studies on clusters of galaxies and large scale structure suggest that the matter density in the Universe should be at least 20% of the critical density ($\Omega_M \gtrsim 0.2$) [19], but the big-bang nucleosynthesis and the measured primordial abundance of helium, deuterium and lithium constrain the baryonic density to $0.01 \lesssim \Omega_b h^2 \lesssim 0.03$ [20]. The anisotropy in the cosmic microwave background radiation measured by the Cosmic Background Explorer (COBE) suggests that at least 60% of the dark matter should be cold (nonrelativistic) [21]. In supersymmetric theories with a conserved R -parity¹, the lightest supersymmetric particle (LSP) cannot decay into normal particles and the LSP is an attractive candidate for cosmological dark matter [22,23]. In most of the supergravity parameter space, the lightest neutralino (χ_1^0) is the LSP [5,11].

Inflationary models usually require $\Omega = 1$ for the Universe [22], although models with $\Omega < 1$ have recently been proposed [24]. Recent measurements on the Hubble constant are converging to $h \simeq 0.6 - 0.7$ [25]. Therefore, we conservatively consider the cosmologically interesting region for $\Omega_{\chi_1^0}$ to be

$$0.1 \lesssim \Omega_{\chi_1^0} h^2 \lesssim 0.5. \quad (2)$$

Following the classic papers of Zel'dovich, Chiu, and Lee and Weinberg [26], many studies of the neutralino relic density in supergravity models have been made with universal [27–30] and nonuniversal [31] soft breaking masses. Recent calculations have taken into account threshold effects and integration over Breit-Wigner poles [32,33]. Previous analyses have focused on the small to moderate $\tan\beta$ range, $\tan\beta \lesssim 25$, but large $\tan\beta$ is equally of interest. Some theoretical models of fermion masses require a large value $\tan\beta$ [34].

In this article, we make more complete calculations of the neutralino relic density over the full range of $\tan\beta$ and SUGRA parameter space with universal GUT scale boundary conditions. We employ the calculational methods of Ref. [30], with some significant improvements.

¹ $R = +1$ for the SM particles and Higgs bosons and $R = -1$ for their superpartners.

The neutralino annihilation cross section is evaluated with helicity amplitude techniques to eliminate any uncertainty from a neutralino velocity expansion. The neutralino relic density is calculated with relativistic Boltzmann averaging, neutralino annihilation threshold effects and Breit-Wigner poles. We introduce a transformation to improve the numerical integration over Breit-Wigner poles and use appropriate extension of the RGEs for large $\tan\beta$ solutions. We determine the constraints on $m_{1/2}$ and $\tan\beta$ implied by Eq. (2). We also impose the constraints from the chargino search at LEP 2 [35]. The effects of the common trilinear coupling (A_0) on A_t , $m_{\tilde{t}_1}$ and the neutralino relic density $\Omega_{\chi_1^0} h^2$ are also studied.

II. RELIC DENSITY OF THE LIGHTEST NEUTRALINO

The present mass density of the lightest neutralino is inversely proportional to the annihilation cross section of χ_1^0 pairs. When kinematically allowed, the neutralino pairs annihilate into fermion pairs ($f\bar{f}$), gauge boson pairs (W^+W^- and ZZ), Higgs boson pairs² (h^0h^0 , H^0H^0 , A^0A^0 , h^0H^0 , h^0A^0 , H^0A^0 and H^+H^-) and associated pairs of gauge and Higgs bosons (Zh^0 , ZH^0 , ZA^0 , and $W^\pm H^\mp$) through s, t, and u channel diagrams. The most convenient approach to calculate the annihilation cross section including interferences among all diagrams is to calculate the amplitude of each diagram with the helicity amplitude formalism³ then numerically evaluate the matrix element squared with a computer. Therefore, following Ref. [30], we employ the HELAS package [36] to calculate the helicity amplitudes. The annihilation cross section of χ_1^0 pairs depends on its mass ($m_{\chi_1^0}$) which we find can be empirically expressed in GeV units as a function of the GUT scale gaugino mass $m_{1/2}$ and $\sin 2\beta$ as

$$\begin{aligned} \mu > 0 : \quad m_{\chi_1^0} &\simeq 0.448m_{1/2} + 11.7 \sin 2\beta - 10.4, \\ \mu < 0 : \quad m_{\chi_1^0} &\simeq 0.452m_{1/2} + 4.68 \sin 2\beta - 12.9, \end{aligned} \quad (3)$$

for $100 \text{ GeV} \lesssim m_{1/2} \lesssim 1000 \text{ GeV}$ and all $\tan\beta$ for which perturbative RGE solutions exist. These neutralino mass formulas hold to an accuracy of $\lesssim 3\%$.

In the regions of Breit-Wigner resonance poles the near-singular amplitudes make the integration unstable. To greatly improve the efficiency and accuracy in calculating the annihilation cross section for processes with a Breit-Wigner resonance, we introduce a transformation $s - M^2 = M\Gamma \tan\theta$ such that [37]

$$\int \frac{ds}{(s - M^2)^2 + (M\Gamma)^2} = \int \frac{d\theta}{M\Gamma} \quad (4)$$

and scale θ to the range (0,1).

The time evolution of the number density $n(t)$ of weakly interacting mass particles is described by the Boltzmann equation [26]

²There are five Higgs bosons: two CP-even h^0 (lighter) and H^0 (heavier), one CP-odd A^0 , and a pair of singly charged H^\pm .

³ The helicity amplitudes of all relevant processes in the non-relativistic limit are given in Ref. [28].

$$\frac{dn}{dt} = -3Hn - \langle\sigma v\rangle [n^2 - n_E^2] \quad (5)$$

where $H = 1.66g_*^{1/2}T^2/M_{Pl}$ is the Hubble expansion rate with $g_* \simeq 81$ the effective number of relativistic degrees of freedom, $M_{Pl} = 1.22 \times 10^{19}$ is the Planck mass, $\langle\sigma v\rangle$ is the thermally averaged cross section times velocity, v is the relative velocity and σ is the annihilation cross section, and n_E is the number density at thermal equilibrium.

In the early Universe, when the temperature $T \gg m_{\chi_1^0}$, the LSP existed abundantly in thermal equilibrium with the LSP annihilations into lighter particles balanced by pair production. Deviation from the thermal equilibrium began when the temperature reached the freeze-out temperature ($T_f \simeq m_{\chi_1^0}/20$). After the temperature dropped well below T_f , the annihilation rate became equal to the expansion rate and $n_{\chi_1^0} = H/\langle\sigma v\rangle$. The resulting relic density can be expressed in terms of the critical density by [22]

$$\Omega_{\chi_1^0} h^2 = m_{\chi_1^0} n_{\chi_1^0} / \rho_c \quad (6)$$

where $n_{\chi_1^0}$ is the number density of χ_1^0 .

The thermally averaged cross section times velocity is

$$\langle\sigma v\rangle(T) = \frac{\int (\sigma v) e^{-E_1/T} e^{-E_2/T} d^3 p_1 d^3 p_2}{\int e^{-E_1/T} e^{-E_2/T} d^3 p_1 d^3 p_2}, \quad (7)$$

where p_1 (E_1) and p_2 (E_2) are the momentum and energy of the two colliding particles in the cosmic, co-moving frame of reference, and T is the temperature. This expression has been simplified to a one-dimensional integral [33] of the form

$$\langle\sigma v\rangle(x) = \frac{1}{4xK_2^2(\frac{1}{x})} \int_2^\infty da \sigma(a) a^2 (a^2 - 4) K_1\left(\frac{a}{x}\right), \quad (8)$$

where $x = \frac{T}{m_{\chi_1^0}}$, $a = \frac{\sqrt{s}}{m_{\chi_1^0}}$, \sqrt{s} is the subprocess energy, and the K_i are modified Bessel functions of order i .

To calculate the neutralino relic density, it is necessary to first determine the scaled freeze-out temperature $x_F \equiv m_{\chi_1^0}/T_f$. The standard procedure is to iteratively solve the freeze out relation

$$x_F^{-1} = \log \left[\frac{m_{\chi_1^0}}{2\pi^3} \sqrt{\frac{45}{2g_* G_N}} \langle\sigma v\rangle_{x_F} x_F^{1/2} \right], \quad (9)$$

starting with $x_F = \frac{1}{20}$. The relic density at the present temperature (T_0) is then obtained from

$$\Omega h^2 = \frac{\rho(T_0)}{8.0992 \times 10^{-47} \text{GeV}^4}, \quad (10)$$

where

$$\rho(T_0) \simeq 1.66 \times \frac{1}{M_{Pl}} \left(\frac{T_{\chi_1^0}}{T_\gamma} \right)^3 T_\gamma^3 \sqrt{g_*} \int_0^{x_F} \langle\sigma v\rangle dx. \quad (11)$$

The ratio $T_{\chi_1^0}/T_\gamma$ is the reheating factor [38] of the neutralino temperature ($T_{\chi_1^0}$) compared to the microwave background temperature (T_γ). The integration in Eq. (11) is evaluated with the modified Bessel functions expanded as power series in x , and then integrated over x . The result is

$$\int_0^{x_F} \langle \sigma v \rangle dx = \frac{1}{\sqrt{8\pi}} \int_2^\infty da \sigma(a) a^{3/2} (a^2 - 4) F(a), \quad (12)$$

where [30]

$$\begin{aligned} F(a) = & \sqrt{\frac{\pi}{a-2}} \left\{ 1 - \text{Erf}f \left(\sqrt{\frac{a-2}{x_F}} \right) \right\} \\ & + 2 \left(\frac{3}{8a} - \frac{15}{4} \right) \left\{ \sqrt{x_F} e^{-\frac{a-2}{x_F}} - \sqrt{\pi(a-2)} \left[1 - \text{Erf}f \left(\sqrt{\frac{a-2}{x_F}} \right) \right] \right\} \\ & + \frac{2}{3} \left(\frac{285}{32} - \frac{45}{32a} - \frac{15}{128a^2} \right) \times \\ & \left\{ e^{-\frac{a-2}{x_F}} \left[x_F^{\frac{3}{2}} - 2(a-2)\sqrt{x_F} \right] + 2\sqrt{\pi}(a-2)^{\frac{3}{2}} \left[1 - \text{Erf}f \left(\sqrt{\frac{a-2}{x_F}} \right) \right] \right\}. \quad (13) \end{aligned}$$

Essentially, all of the contribution to the integral in Eq. (12) comes from $a < 2.5$.

To generate the SUSY particle mass spectrum and couplings for the neutralino relic density calculation, we run the gauge coupling RGEs from the weak scale up to a high energy scale⁴ to fix the unification scale M_{GUT} , and the unified gauge coupling α_{GUT} . Then we run all the RGEs from M_{GUT} to the weak scale of M_Z . The SUSY mass scale (M_{SUSY}) is chosen to be 2 TeV; closely similar results are obtained with a 1 TeV mass scale.

In Figure 1, we present masses, in the case⁵ $\mu > 0$, for the lightest neutralino (χ_1^0), the lighter top squark (\tilde{t}_1), the lighter tau slepton ($\tilde{\tau}_1$), and two neutral Higgs bosons: the lighter CP-even (h^0) and the CP-odd (A^0). To a good approximation, the mass of the lightest chargino (χ_1^\pm) is about twice $m_{\chi_1^0}$ and the mass of the heavier CP-even Higgs boson (H^0) is close to m_A [5,11]. For $m_0 \sim 100$ GeV and $m_{1/2} \gtrsim 400$ GeV, the mass of $\tilde{\tau}_1$ can become smaller than $m_{\chi_1^0}$ so such regions are theoretically excluded. Also shown in Fig. 1 are the regions that do not satisfy the following theoretical requirements: electroweak symmetry breaking (EWSB), tachyon free, and the lightest neutralino as the LSP. The region excluded by the $m_{\chi_1^\pm} > 85$ GeV limit from the chargino search [35] at LEP 2 is indicated. Masses for $\mu < 0$ are shown in Fig. 2.

There are several interesting aspects to note in Figs. 1 and 2:

- (i) For $\tan \beta \sim 1.8$, $\mu > 0$ generates heavier neutralinos and charginos but lighter h^0 than

⁴ For simplicity, we employed the one-loop RGEs in our analysis since the two-loop modifications to the SUSY mass spectra are only a few percent of the one-loop RGE results [5]. We did not include heavy particle threshold effects in the RGE evolution, which may introduce small corrections when $\tan \beta$ is large [39].

⁵ Our convention for the sign of μ follows that of Ref. [5] and is opposite to that of Ref. [30]; see Eq. (1).

$\mu < 0$ for the same $m_{1/2}$ and m_0 .

(ii) An increase in $\tan\beta$ leads to a larger m_h but a reduction in $m_{\chi_1^0}$, $m_{\chi_1^\pm}$, m_A and m_H .

(iii) For $\tan\beta \sim 50$, $m_A \sim m_H$ can become comparable to $m_{\chi_1^0}$.

(iv) Increasing m_0 raises m_A , m_H and the masses of other scalars significantly.

The relic density of the neutralino dark matter ($\Omega_{\chi_1^0} h^2$) for the case $\mu > 0$ is presented in Fig. 3 versus $m_{1/2}$ for several values of m_0 and $\tan\beta$. Figure 4 shows similar contours for $\mu < 0$. When $2m_{\chi_1^0}$ is close to the mass of Z , h^0 , H^0 , or A^0 , the cross section is significantly enhanced by the Breit-Wigner resonance pole, and a corresponding dip appears in the relic density distribution. For $\mu > 0$, $\tan\beta = 1.8$ and $m_0 = 100$ GeV, there are two dips, the first one occurs at the h^0 pole ($m_{1/2} = 55$ GeV, $m_{\chi_1^0} = 26$ GeV and $m_h = 52$ GeV), and the second one appears at the Z pole ($m_{1/2} \simeq 100$ GeV and $m_{\chi_1^0} = 45$ GeV $\sim \frac{1}{2}M_Z$). An increase in m_0 raises the mass of Higgs bosons but does not affect the mass of χ_1^0 . Therefore, comparing the $m_0 = 100$ GeV results to those of $m_0 = 500$ GeV, the Z -pole dips occur at about the same $m_{1/2}$ as above, but the h -pole dips appear at larger $m_{1/2}$ and $m_{\chi_1^0}$. Increasing $\tan\beta$ slightly raises m_h , slightly lowers $m_{\chi_1^0}$, and greatly reduces m_A and m_H . For $\tan\beta \sim 45$, extra dips appear in Figs. 3(c) and 4(c). These resonance dips are associated with the A^0 and H^0 masses and occur where $2m_{\chi_1^0} \simeq m_A \simeq m_H$. For $\tan\beta \leq 10$ and $m_0 > 200$ GeV, the annihilation cross section is too small for a cosmologically interesting $\Omega_{\chi_1^0} h^2$, while for $\tan\beta \sim 45$, m_0 must be close to 1000 GeV for $m_{1/2} \lesssim 750$ GeV and be larger than 400 GeV for $m_{1/2} \gtrsim 750$ GeV to obtain an interesting relic density. For $\tan\beta \gtrsim 50$, $m_A \lesssim 2m_{\chi_1^0}$, and there are no A^0 and H^0 resonant contributions; an acceptable Ωh^2 is found for $m_0 \gtrsim 400$ GeV and 400 GeV $\lesssim m_{1/2} \lesssim 800$ GeV.

III. CONSTRAINTS ON THE SUGRA PARAMETER SPACE

To show the constraints of Eq. (2) on the SUGRA parameter space, we present contours of $\Omega_{\chi_1^0} h^2 = 0.1$ and 0.5 in the $(m_{1/2}, \tan\beta)$ plane in Fig. 5 for $\mu > 0$. Also shown are the regions that do not satisfy the theoretical requirements (electroweak symmetry breaking, tachyon free, and lightest neutralino as the LSP) and the region excluded by the chargino search ($m_{\chi_1^\pm} < 85$ GeV) at LEP 2 [35]. Figure 6 shows similar contours for $\mu < 0$.

We summarize below the central features of these results.

If m_0 is close to 100 GeV,

- Most of the $(m_{1/2}, \tan\beta)$ plane with $\tan\beta \gtrsim 40$ is excluded by the above mentioned theoretical requirements.
- The chargino search at LEP 2 excludes the region where $m_{1/2} \lesssim 100$ GeV for $\mu > 0$ and $m_{1/2} \lesssim 120$ GeV for $\mu < 0$.
- The cosmologically interesting region is 100 GeV $\lesssim m_{1/2} \lesssim 400$ GeV and $\tan\beta \lesssim 25$ for either sign of μ .

If m_0 is close to 500 GeV,

- Most of the $(m_{1/2}, \tan\beta)$ plane is theoretically acceptable for $\tan\beta \lesssim 50$ and $m_{1/2} \gtrsim 120$ GeV.

- The LEP 2 chargino search excludes (i) $m_{1/2} \lesssim 140$ GeV for $\tan\beta \gtrsim 10$, and (ii) $m_{1/2} \lesssim 80$ GeV ($\mu > 0$) or $m_{1/2} \lesssim 120$ GeV ($\mu < 0$) for $\tan\beta \sim 1.8$.
- The cosmologically interesting regions lie in two narrow bands.

Contours of $\Omega_{\chi_1^0} h^2 = 0.1$ and 0.5 in the $(m_{1/2}, m_0)$ plane are presented in Fig. 7 for $\mu > 0$ with $\tan\beta = 1.8$ and 50 . Also shown are the theoretically excluded regions. Figure 8 shows similar contours for $\mu < 0$. Salient features of these results are summarized in the following. If $\tan\beta$ is close to 1.8 ,

- Most of the $(m_{1/2}, m_0)$ parameter space is theoretically acceptable.
- The chargino search at LEP 2 excludes the region where $m_{1/2} \lesssim 80$ GeV for $\mu > 0$ and $m_{1/2} \lesssim 110$ GeV for $\mu < 0$.
- Most of the cosmologically interesting region is 80 GeV $\lesssim m_{1/2} \lesssim 450$ GeV and $m_0 \lesssim 200$ GeV.

If $\tan\beta$ is close to 50 ,

- The theoretically acceptable region in the $(m_{1/2}, m_0)$ plane is constrained to have $m_0 \gtrsim 160$ GeV and $m_{1/2} \gtrsim 150$ GeV for $\tan\beta \sim 50$.
- The LEP 2 chargino search excludes (i) the region with $m_{1/2} \lesssim 125$ GeV for $\mu > 0$ or (ii) the region with $m_{1/2} \lesssim 135$ GeV for $\mu < 0$, which is already inside the theoretically excluded region.
- The cosmologically interesting region lies in a band with (i) 475 GeV $\lesssim m_{1/2} \lesssim 800$ GeV for $\mu > 0$, or (ii) 500 GeV $\lesssim m_{1/2} \lesssim 840$ GeV for $\mu < 0$, and $m_0 \gtrsim 300$ GeV.

To correlate the acceptable values of neutralino relic density to the masses of SUSY particles at the weak scale, we present $\Omega_{\chi_1^0} h^2$ and representative SUSY mass spectra versus $m_{1/2}$ in Fig. 9, for $\mu > 0$ with (a) $\tan\beta = 1.8$, $m_0 = 150$ GeV and (b) $\tan\beta = 50$, $m_0 = 600$ GeV. Figure 10 shows similar contours for $\mu < 0$. Also shown are the theoretically excluded regions and the excluded region from the chargino search at LEP 2.

The neutralino relic density and representative SUSY mass spectrum versus m_0 are presented in Fig. 11, for $\mu > 0$ with (a) $\tan\beta = 1.8$, $m_{1/2} = 150$ GeV and (b) $\tan\beta = 50$, $m_{1/2} = 500$ GeV. Figure 12 shows similar contours for $\mu < 0$. Also shown are the theoretically excluded regions.

The foregoing results were based on the GUT scale trilinear coupling choice $A_0 = 0$. To examine the sensitivity of the results to A_0 , we present the neutralino relic density versus A_0 in Fig. 13 for various values of $m_0 = m_{1/2}$ and $\tan\beta$. For $\tan\beta \lesssim 10$, $\Omega_{\chi_1^0} h^2$ is almost independent of A_0 . For $\tan\beta \sim 40$, the relic density is reduced by a positive A_0 but enhanced by a negative A_0 . Significant impact of A_0 on $\Omega_{\chi_1^0} h^2$ occurs only when both m_0 and $m_{1/2}$ are small and $\tan\beta$ is large. For $m_0 = m_{1/2} = 200$ GeV and $\tan\beta = 40$ the theoretically allowed range of A_0 is -380 GeV $\lesssim A_0 \lesssim 590$ GeV. The value of $\Omega_{\chi_1^0} h^2$ with $A_0 = 590$ GeV (-380 GeV) is about 0.22 (2.4) times the value with $A_0 = 0$. For $m_0 = m_{1/2} = 800$ GeV and $\tan\beta = 40$ the value of $\Omega_{\chi_1^0} h^2$ with $A_0 = 1000$ GeV (-1000 GeV) is about 0.58 (1.7) times the value with $A_0 = 0$.

The dependence of $\Omega_{\chi_1^0} h^2$ on A_0 occurs because the masses of top squarks are sensitive to A_t , and the t-channel diagrams involving the stops make important contribution to neutralino annihilation cross section. In figures 14 ($\mu > 0$) and 15 ($\mu < 0$), we show the mass of the lighter top squark ($m_{\tilde{t}_1}$) and the trilinear coupling A_t versus A_0 for various values of $m_0 = m_{1/2}$ and $\tan\beta$. The trilinear coupling A_t is always negative and it is nearly a linear function of A_0 . For $\tan\beta$ close to the top Yukawa infrared fixed point, $\tan\beta \simeq 1.8$, A_t approaches an infrared fixed point value as well, $A_t \simeq -1.7m_{1/2}$, to about 30% accuracy, independent of the value of A_0 [40].

IV. CONCLUSIONS

The existence of dark matter in the Universe provides a potentially important bridge between particle physics and cosmology. Within SUGRA GUTs, the lightest neutralino is the most likely dark matter candidate. We evaluated the neutralino relic density using helicity amplitude methods including all relevant diagrams. We applied a transformation to improve the efficiency and accuracy of annihilation cross section calculations in regions with Breit-Wigner resonance poles. Requiring that the neutralino relic density should be in the cosmologically interesting region, we were able to place tight constraints on the SUGRA parameter space, especially in the plane of $m_{1/2}$ versus $\tan\beta$, since the mass of the lightest neutralino depends mainly on these two parameters. We derived empirical formulas relating $m_{\chi_1^0}$ to $m_{1/2}$ and $\sin\beta$. The cosmologically interesting regions of the parameter space with $\tan\beta$ close to the top Yukawa infrared fixed points are found to be

$$\begin{aligned} \tan\beta = 1.8 : \quad & 80 \text{ GeV} \lesssim m_{1/2} \lesssim 450 \text{ GeV} \text{ and } m_0 \lesssim 200 \text{ GeV} \\ \tan\beta = 50 : \quad & 500 \text{ GeV} \lesssim m_{1/2} \lesssim 800 \text{ GeV} \text{ and } m_0 \gtrsim 300 \text{ GeV} \end{aligned}$$

where the high $\tan\beta$ result is based on $A_0 = 0$. Both regions are nearly independent of the sign of μ . We presented expectations for the SUSY particle mass spectra corresponding to these regions of parameter space. For the IRFP at $\tan\beta = 1.8$, the lighter scalar tau ($\tilde{\tau}_1$) and the lightest scalar neutrino ($\tilde{\nu}$) can be relatively light ($\lesssim 200$ GeV) in the cosmologically interesting region.

For $\tan\beta \lesssim 10$, the neutralino relic density $\Omega_{\chi_1^0} h^2$ is almost independent of the trilinear couplings A_0 . For $\tan\beta \sim 40$, the relic density is reduced by a positive A_0 while enhanced by a negative A_0 . The value of A_0 significantly affects $\Omega_{\chi_1^0} h^2$ only when $\tan\beta$ is large and both m_0 and $m_{1/2}$ are small.

Supernovae [41], cosmic microwave background [42] and other astronomical observations will soon provide precise information on the Hubble parameter h and the cold dark matter component of Ω . This information will pinpoint the SUGRA GUT parameters, which in turn predict the SUSY particle masses in these models.

ACKNOWLEDGMENTS

We are grateful to Howie Baer and Michal Brhlik for providing us with their computer code, and to Mike Berger, Gary Steigman and Dieter Zeppenfeld for valuable discussions. We thank Manuel Drees for beneficial comments regarding the choice of scale for the one-loop effective potential. This research was supported in part by the U.S. Department of Energy under Grant No. DE-FG02-95ER40896, and in part by the University of Wisconsin Research Committee with funds granted by the Wisconsin Alumni Research Foundation.

REFERENCES

- [1] K. Inoue, A. Kakuto, H. Komatsu and H. Takeshita, *Prog. Theor. Phys.* **68**, 927 (1982) and **71**, 413 (1984).
- [2] H.P. Nilles, *Phys. Rep.* **110**, 1 (1984); H. Haber and G. Kane, *Phys. Rep.* **117**, 75 (1985).
- [3] For recent reviews, see X. Tata, in *The Standard Model and Beyond*, edited by J.E. Kim, (World Scientific, Singapore, 1991); TASI-95 lectures, University of Hawaii Report No. UH-511-833-95 (1995).
- [4] M.S. Chanowitz, J. Ellis and M.K. Gaillard, *Nucl. Phys.* **B128**, 506 (1977).
- [5] V. Barger, M.S. Berger, P. Ohmann, *Phys. Rev. D* **47**, 1093 (1993); *Phys. Rev. D* **49**, 4908 (1994); V. Barger, M.S. Berger, P. Ohmann and R.J.N. Phillips, *Phys. Lett. B* **314**, 351 (1993).
- [6] B. Pendleton and G.G. Ross, *Phys. Lett. B* **98**, 291 (1981); C.T. Hill, *Phys. Rev. D* **24**, 691 (1981).
- [7] C.D. Froggatt, R.G. Moorhouse and I.G. Knowles, *Phys. Lett. B* **298**, 356 (1993).
- [8] J. Bagger, S. Dimopoulos and E. Masso, *Phys. Rev. Lett.* **55**, 920 (1985); H. Arason, *et al.*, *Phys. Rev. Lett.* **67** 2933 (1991); and *Phys. Rev. D* **46**, 3945 (1992); P. Langacker, N. Polonsky, *Phys. Rev. D* **50**, 2199 (1994); W.A. Bardeen, M. Carena, S. Pokorski and C.E.M. Wagner, *Phys. Lett. B* **320**, 110 (1994); M. Carena, M. Olechowski, S. Pokorski and C.E.M. Wagner *Nucl. Phys. B* **419**, 213 (1994); M. Carena and C.E.M. Wagner, *Nucl. Phys. B* **452**, 45 (1995); B. Schrepf, *Phys. Lett. B* **344** (1995) 193; B. Schrepf and M. Wimmer, DESY-96-109 (1996), hep-ph/9606386, and references therein.
- [9] A.H. Chamseddine, R. Arnowitt and P. Nath, *Phys. Rev. Lett.* **49**, 970 (1982); L. Ibañez and G. Ross, *Phys. Lett.* **B110**, 215 (1982); L. Ibañez, *Phys. Lett.* **B118**, 73 (1982); J. Ellis, D. Nanopoulos and K. Tamvakis, *Phys. Lett.* **B121**, 123 (1983); L. Alvarez-Gaumé, J. Polchinski and M. Wise, *Nucl. Phys.* **B121**, 495 (1983).
- [10] V. Berezhinskii, *et al.*, *Astropart. Phys.* **5**, 1 (1996); P. Nath and R. Arnowitt, Northeastern Report No. NUB-TH-3151-97, (1997), hep-ph/9701301.
- [11] J. Ellis and F. Zwirner, *Nucl. Phys.* **B338**, 317 (1990); G. Ross and R.G. Roberts, *Nucl. Phys.* **B377**, 571 (1992); R. Arnowitt and P. Nath, *Phys. Rev. Lett.* **69**, 725 (1992); M. Drees and M.M. Nojiri, *Nucl. Phys.* **B369**, 54 (1993); S. Kelley *et al.*, *Nucl. Phys.* **B398**, 3 (1993); M. Olechowski and S. Pokorski, *Nucl. Phys.* **B404**, 590 (1993); G. Kane, C. Kolda, L. Roszkowski and J. Wells, *Phys. Rev.* **D49**, 6173 (1994); D.J. Castaño, E. Piard and P. Ramond, *Phys. Rev.* **D49**, 4882 (1994); W. de Boer, R. Ehret and D. Kazakov, *Z. Phys.* **67**, 647 (1995); H. Baer, M. Drees, C. Kao, M. Nojiri

- and X. Tata, Phys. Rev. D **50**, 2148 (1994); H. Baer, C.-H. Chen, R. Munroe, F. Paige and X. Tata, Phys. Rev. D **51**, 1046 (1995).
- [12] M.S. Alam et al., (CLEO Collaboration), Phys. Rev. Lett. **74**, 2885 (1995).
- [13] P.G. Colrain and M.I. Williams, talk presented at the International Europhysics Conference on High Energy Physics, Jerusalem, Israel, August 1997.
- [14] P. Nath and R. Arnowitt, Phys. Lett. B **336**, 395 (1994); Phys. Rev. Lett. **74**, 4592 (1995); Phys. Rev. D **54**, 2374 (1996); F. Borzumati, M. Drees and M. Nojiri, Phys. Rev. D **51**, 341 (1995); H. Baer and M. Brhlik, Phys. Rev. D **55**, 3201 (1997). and references therein.
- [15] H. Haber and R. Hempfling, Phys. Rev. Lett. **66** (1991) 1815; J. Ellis, G. Ridolfi and F. Zwirner, Phys. Lett. B **257**, 83 (1991); T. Okada, H. Yamaguchi and T. Tanagida, Prog. Theor. Phys. Lett. **85**, 1 (1991); We use the calculations of M. Bisset, Ph.D. thesis, University of Hawaii (1994).
- [16] H. Baer, C.-H. Chen, M. Drees, F. Paige and X. Tata, Florida State University Report No. FSU-HEP-970501, hep-ph/9704457.
- [17] M. Carena, J.R. Espinosa, M. Quiros, and C.E.M. Wagner, Phys. Lett. B **355**, 209 (1995); M. Carena, M. Quiros, C.E.M. Wagner, Nucl. Phys. **B461**, 407 (1996); H. Haber, R. Hempfling and A. Hoang, CERN-TH/95-216 (1996), hep-ph/9609331.
- [18] For reviews on dark matter and its detection, see *e. g.*, V. Trimble, Annu. Rev. Astron. Astrophys. **25**, 425 (1987); J.R. Primack, B. Sadoulet and D. Seckel, Annu. Rev. Nucl. Part. Sci. **38**, 751 (1988); P.F. Smith and J.D. Lewin, Phys. Rep. **187**, 203 (1990).
- [19] A. Dekel and M.J. Rees, *Astrophys. J.* **422**, L1 (1994); A. Dekel, Annu. Rev. Astron. Astrophys. **32**, 371 (1994); M. Strauss and J. Willick, Phys. Rep. **261**, 271 (1995); N. Bahcall, L.M. Lubin and V. Dorman, *Astrophys. J.* **447**, L81 (1995); R.G. Carlberg, H.K.C. Yee, and E. Ellingson, astro-ph/9512087. For a review and recent developments, see A. Dekel, D. Burstein, and S. White, talk presented at Conference on Critical Dialogs in Cosmology, Princeton, NJ, June (1996), astro-ph/9611108.
- [20] T.P. Walker, G. Steigman, D.N. Schramm, K.A. Olive and H-S. Kang, *Astrophys. J.* **376** (1991) 51; M.S. Smith, L.H. Kawano and R.A. Malaney, *Astrophys. J. Suppl. Ser.* **85** (1993) 219; C.J. Copi, D.N. Schramm and M.S. Turner, *Science* **267**, 192 (1995).
- [21] M. White, D. Scott and J. Silk, *Annu. Rev. Astron. Astrophys.* **32**, 319 (1994).
- [22] E.W. Kolb and M.S. Turner, *The Early Universe*, (Addison-Wesley, Redwood City, CA, 1989).
- [23] For reviews, see G. Jungman, M. Kamionkowski and K. Griest, Phys. Rep. **267** (1996) 195; P. Nath and R. Arnowitt, presented at the International Workshop on Aspects of Dark Matter in Astrophysics and Particle Physics, Heidelberg, Germany, Sep 1996, hep-ph/9610460; M. Drees, invited talk at 12th DAE Symposium on High-Energy Physics, Guahati, India, Dec 1996, hep-ph/9703260; and references therein.
- [24] M. Bucher, A.S. Goldhaber, and N. Turok, Phys. Rev. D **52**, 3314 (1995); A.D. Linde and A. Mezhlumian, *ibid* **52**, 6789 (1995); J.R. Gott, *Nature*, **295**, 304 (1992).
- [25] A.G. Riess, R.P. Krishner, and W.H. Press, *Astrophys. J.* **438**, L17 (1995); *Astrophys. J.* **473**, 88 (1996); D. Branch, A. Fisher, E. Baron, P. Nugent, *Astrophys. J.* **470**, L7 (1996); W. Freedman, talk presented at Conference on Critical Dialogs in Cosmology, Princeton, NJ, June (1996), astro-ph/9612024; R. Giovanelli *et al.*, astro-ph/9612072.
- [26] Ya.B. Zel'dovich, *Adv. Astron. Astrophys.*, **3**, 241 (1965); H.-Y. Chiu, Phys. Rev. Lett.

- 17**, 712 (1966); B. Lee and S. Weinberg, Phys. Rev. Lett. **39**, 165 (1977).
- [27] R. Barbieri, M. Frigeni and G.F. Giudice, Nucl. Phys. B **313**, 725 (1989); J.L. Lopez, D.V. Nanopoulos and K.-J. Yuan, Phys. Lett. B **267**, 219 (1991) and Nucl. Phys. **B370**, 445 (1992); J. Ellis and L. Roszkowski, Phys. Lett. B **283**, 252 (1992); L. Roszkowski and R. Roberts, Phys. Lett. B **309**, 329 (1993); M. Kawasaki and S. Mizuta, Phys. Rev. D **46**, 1634 (1992); G.L. Kane, C. Kolda, L. Roszkowski and J.D. Wells, Phys. Rev. D **49**, 6173 (1994); E. Diehl, G.L. Kane, C. Kolda and J.D. Wells, Phys. Rev. D **52**, 4223 (1995).
- [28] M. Drees and M.M. Nojiri, Phys. Rev. D **47**, 376 (1993).
- [29] R. Arnowitt and P. Nath, Phys. Lett. B **299**, 58 (1993); B **307**, 403(E) (1993); Phys. Rev. Lett. **70**, 3696 (1993); Phys. Rev. D **54**, 2374 (1996); J.L. Lopez, D.V. Nanopoulos and K. Yuan, Phys. Rev. D **48**, 2766 (1993); M. Drees and A. Yamada, Phys. Rev. D **53**, 1586 (1996); J. Ellis, T. Falk, K.A. Olive and M. Schmitt, Phys. Lett. B **388**, 97 (1996); CERN Report No. CERN-TH-97-105, hep-ph/9705444.
- [30] H. Baer and M. Brhlik, Phys. Rev. D **53**, 597 (1996).
- [31] D. Matalliotakis and H.P. Nilles, Nucl. Phys. B **435**, 115 (1995); M. Olechowski and S. Pokorski, Phys. Lett. B **344**, 201 (1995); V. Berezinskii, A. Bottino, J. Ellis (CERN), N. Fornengo, G. Mignola, S. Scopel, Astropart. Phys. **5**, 1 (1996); P. Nath and R. Arnowitt, Phys. Rev. **D56**, 2820 (1997).
- [32] K. Griest and D. Seckel, Phys. Rev. D **43**, 3191 (1991).
- [33] P. Gondolo and G. Gelmini, Nucl. Phys. **B360**, 145 (1991).
- [34] G. Anderson, S. Raby, S. Dimopoulos, and L.J. Hall, Phys. Rev. D **49**, 3660 (1994); S. Dimopoulos, L.J. Hall and S. Raby, Phys. Rev. D **45**, 4192 (1992); Phys. Rev. Lett. **68**, 1984 (1992).
- [35] ALEPH collaboration, talk presented at CERN by G. Cowan, February (1997).
- [36] HELAS: HELicity Amplitude Subroutines for Feynman Diagram Evaluations, H. Murayama, I. Watanabe and K. Hagiwara, KEK-91-11 (1992).
- [37] V. Barger and R. Phillips, *Collider Physics, updated edition*, (Addison-Wesley Publishing Company, Redwood City, CA, 1997).
- [38] J. Ellis, J. Hagelin, D. Nanopoulos, K. Olive and M. Srednicki, Nucl. Phys. **B238**, 453 (1984).
- [39] T. Blazek and S. Raby, Phys. Lett. B **392**, 371 (1997); T. Blazek, M. Carena, S. Raby and C.E.M. Wagner, Ohio State Report No. OHSTPY-HEP-T-96-026, hep-ph/9611217.
- [40] M. Carena, M. Olechowski, S. Pokorski and C.E.M. Wagner, Nucl. Phys. B **419**, 213 (1994).
- [41] S. Perlmutter, *et al.*, LBL-39291, (1996), astro-ph/9608192.
- [42] C.H. Lineweaver, D. Barbosa, A. Blanchard and J.G. Bartlett, astro-ph/9610133; M. Zaldarriaga, D.N. Spergel and U. Seljak, astro-ph/9702157.

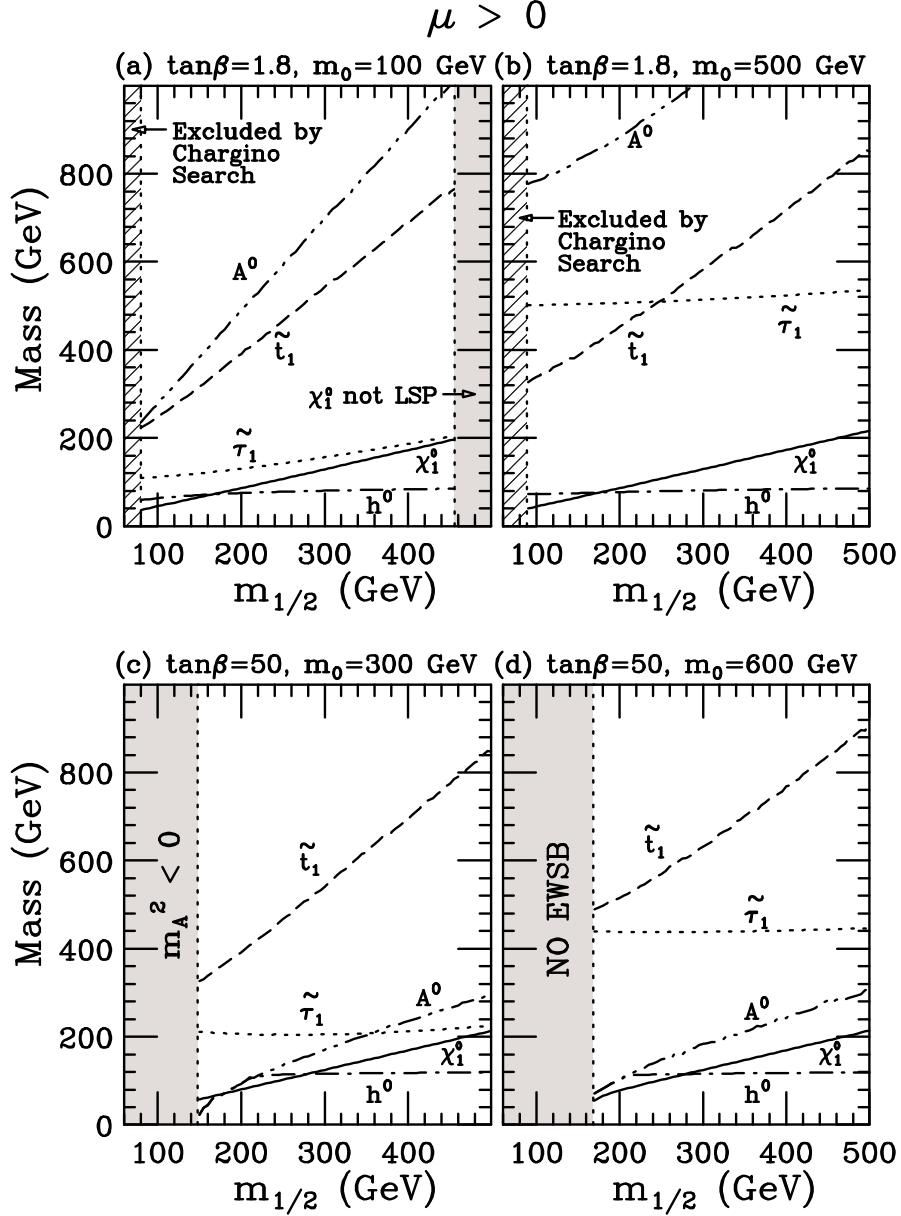


FIG. 1. Masses of χ_1^0 , \tilde{t}_1 , $\tilde{\tau}_1$ at the mass scale of M_Z and masses of h^0 , and A^0 at the mass scale $Q = \sqrt{m_{\tilde{t}_L} m_{\tilde{t}_R}}$, versus $m_{1/2}$, with $M_{\text{SUSY}} = 2$ TeV and $\mu > 0$ for (a) $\tan\beta = 1.8$, $m_0 = 100$ GeV, (b) $\tan\beta = 1.8$, $m_0 = 500$ GeV, (c) $\tan\beta = 50$, $m_0 = 300$ GeV, and (d) $\tan\beta = 50$, $m_0 = 600$ GeV. The shaded regions are excluded by theoretical requirements (EWSB, tachyons, LSP), or the chargino search at LEP 2.

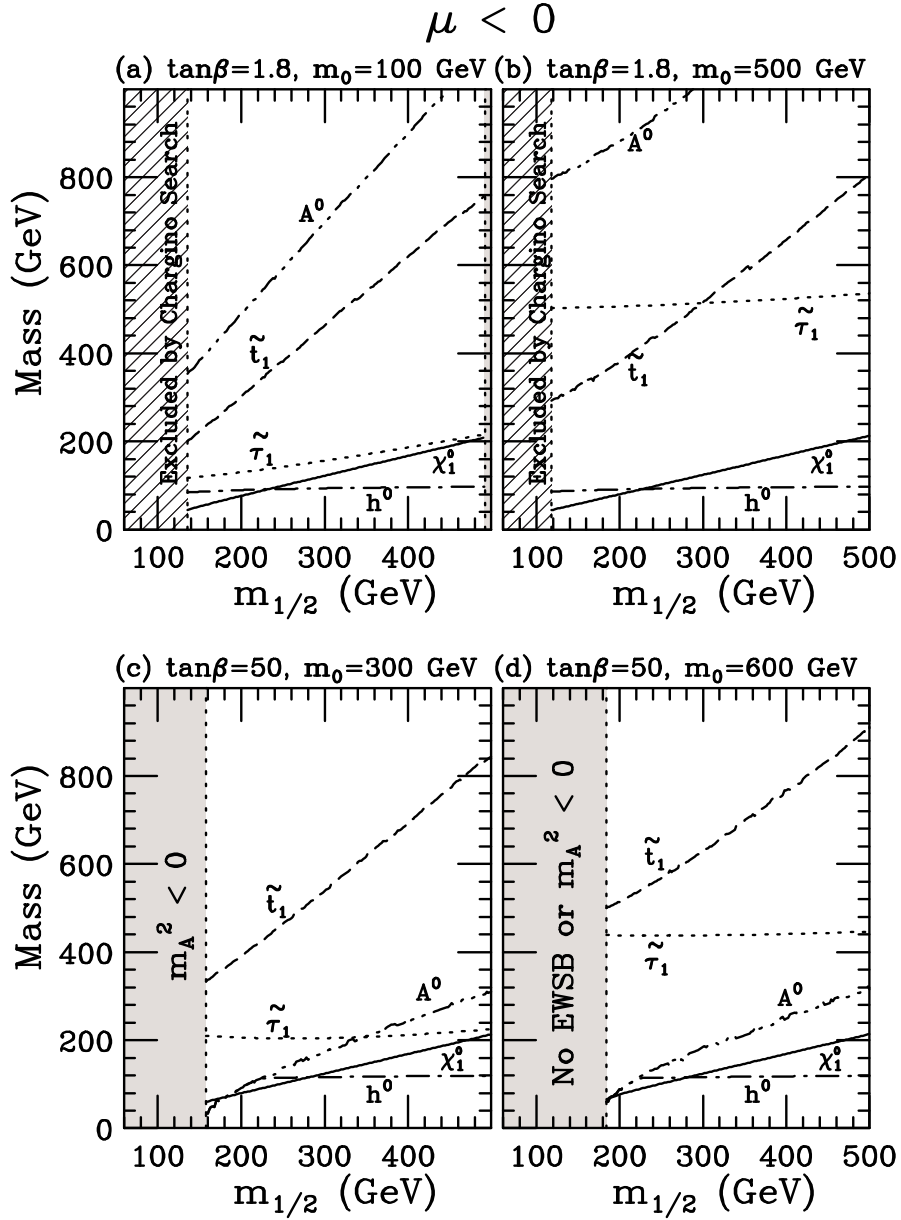


FIG. 2. The same as in Fig. 1, except that $\mu < 0$.

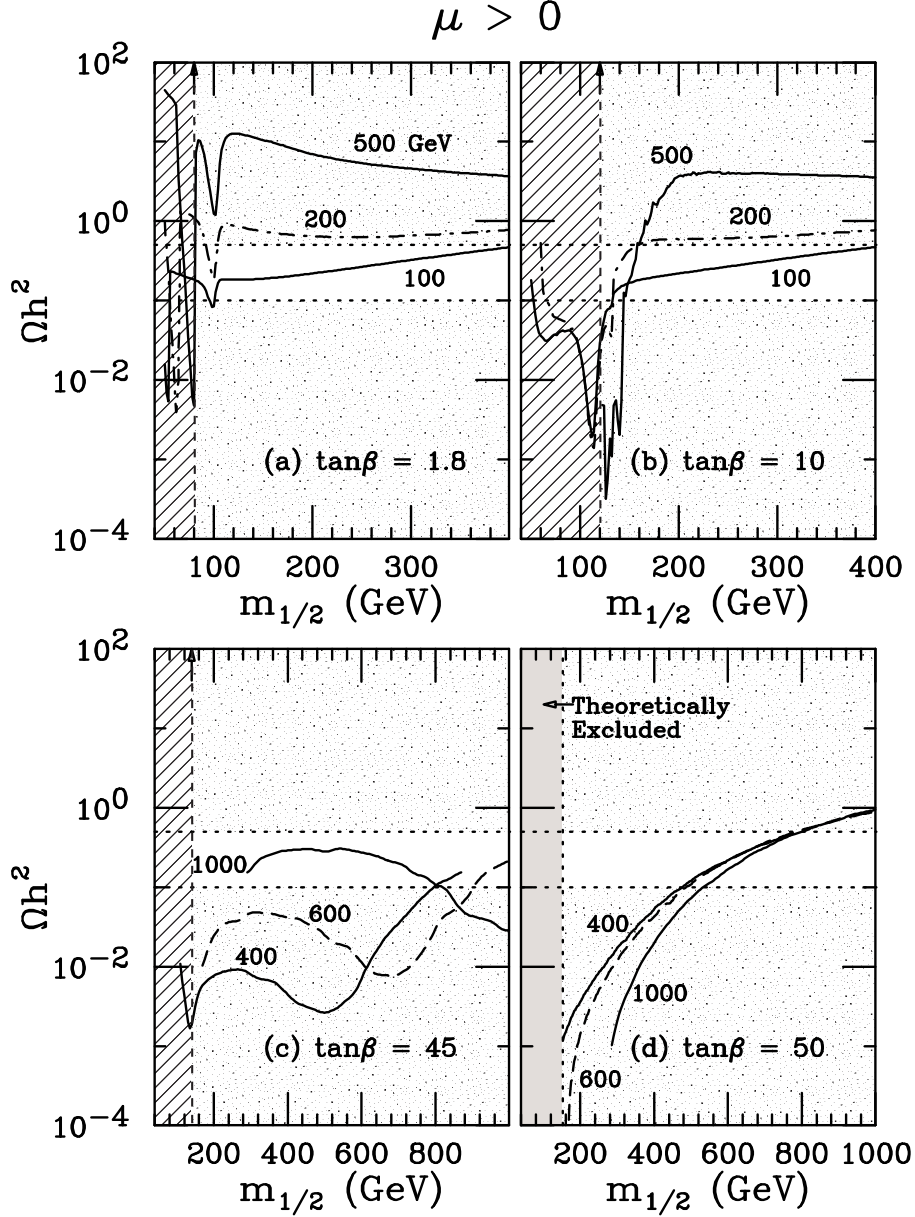


FIG. 3. $\Omega_{\chi_1} h^2$ versus $m_{1/2}$ for $\mu > 0$, with representative values of m_0 and (a) $\tan\beta = 1.8$, (b) $\tan\beta = 10$, (c) $\tan\beta = 45$, and (d) $\tan\beta = 50$. The shaded regions denote the parts of the parameter space (i) producing $\Omega_{\chi_1} h^2 < 0.1$ or $\Omega_{\chi_1} h^2 > 0.5$, (ii) excluded by theoretical requirements, or (iii) excluded by the chargino search at LEP 2.

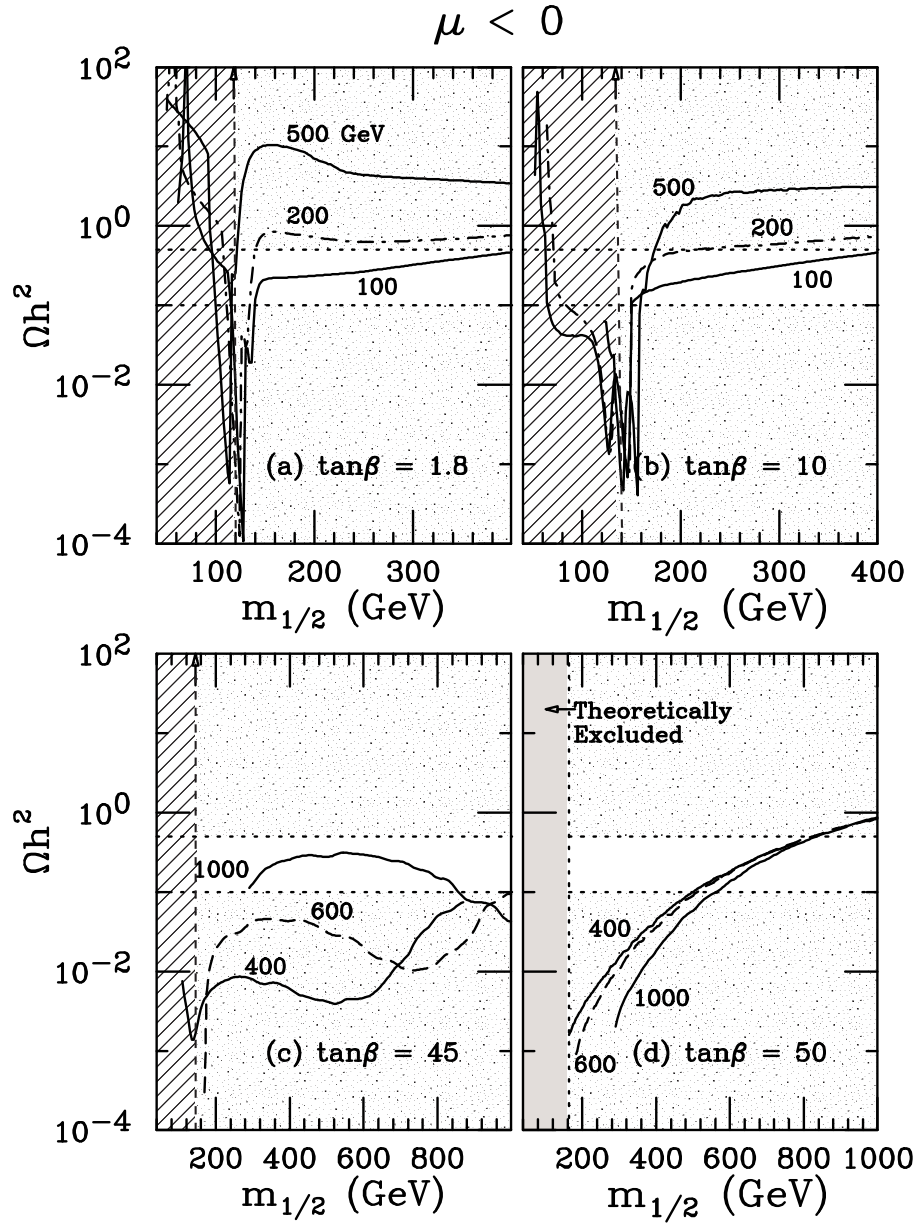


FIG. 4. The same as in Fig. 3, except that $\mu < 0$.

Contours of Ωh^2 for $\mu > 0$

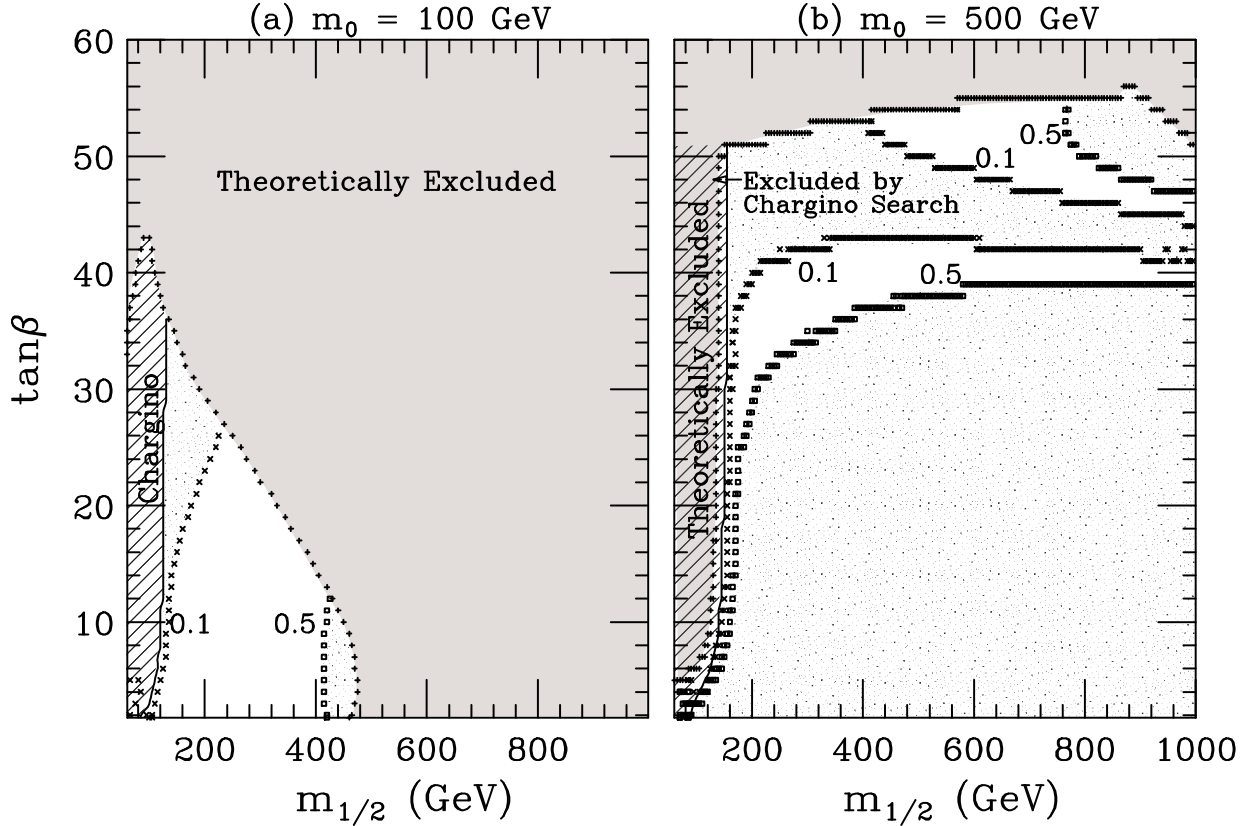


FIG. 5. Contours of $\Omega_{\chi_1^0} h^2 = 0.1$ and 0.5 in the $(m_{1/2}, \tan\beta)$ plane, for $\mu > 0$, (a) $m_0 = 100$ GeV and (b) $m_0 = 500$ GeV. The shaded regions denote the parts of the parameter space (i) producing $\Omega_{\chi_1^0} h^2 < 0.1$ or $\Omega_{\chi_1^0} h^2 > 0.5$, (ii) excluded by theoretical requirements, or (iii) excluded by the chargino search at LEP 2.

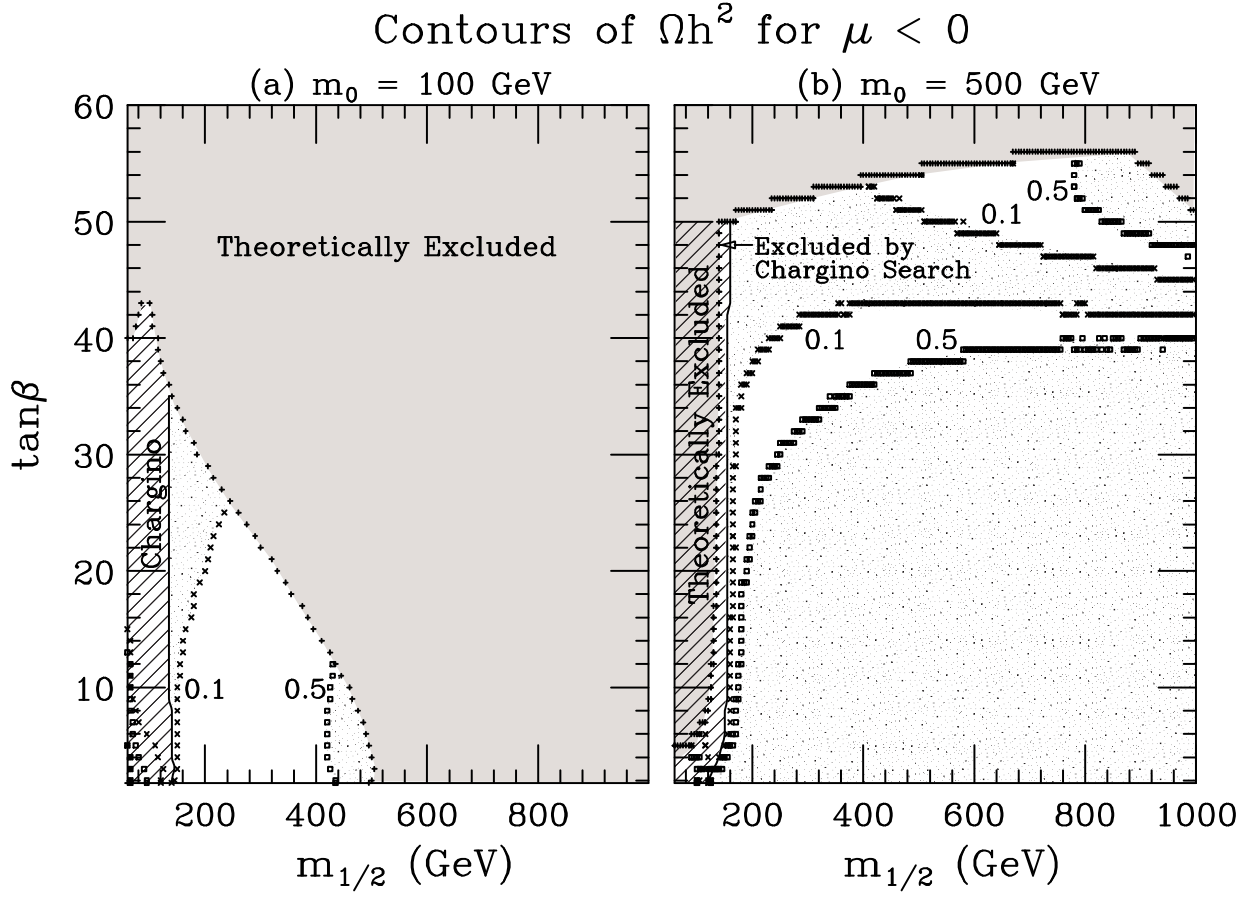


FIG. 6. The same as in Fig. 5, except that $\mu < 0$.

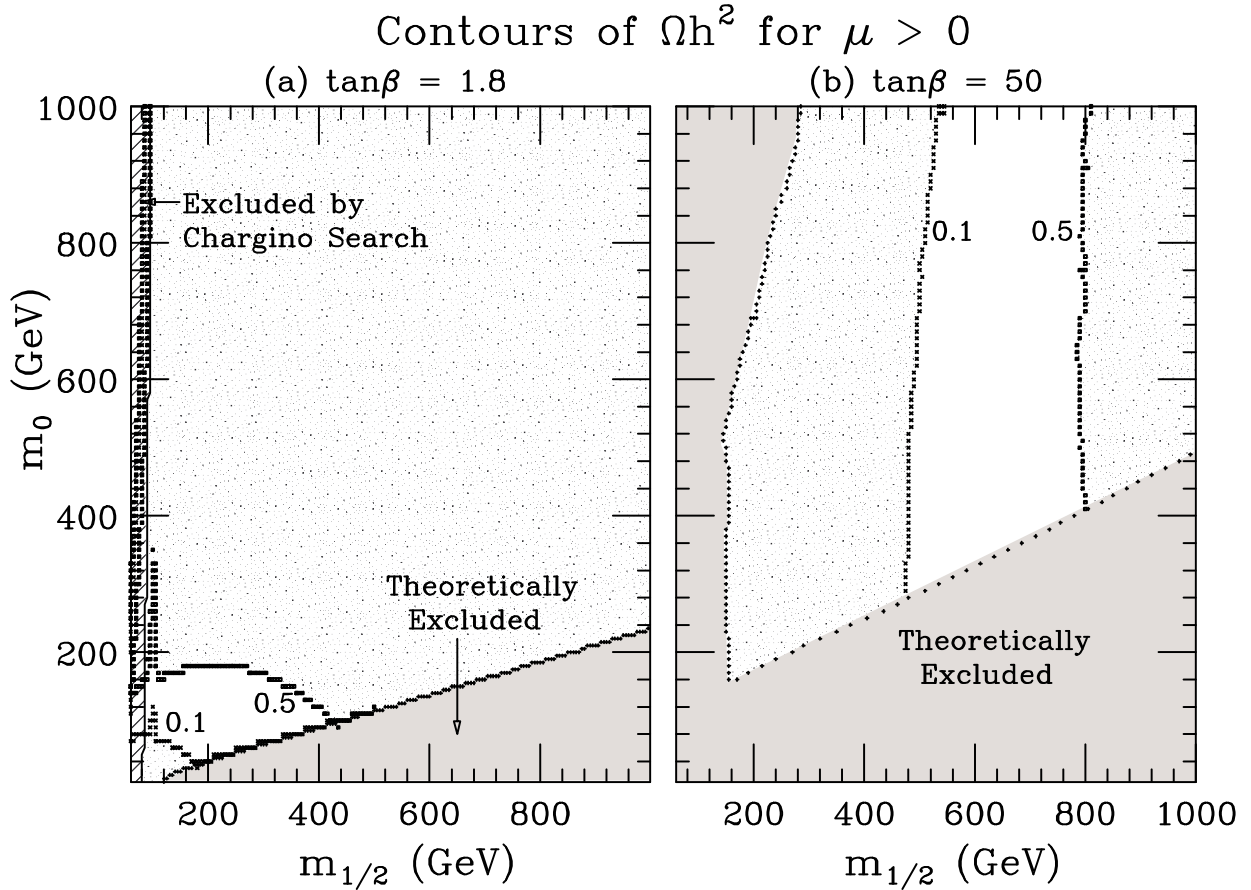


FIG. 7. Contours of $\Omega_{\chi_1^0} h^2 = 0.1$ and 0.5 in the $(m_{1/2}, m_0)$ plane, for $\mu > 0$, (a) $\tan\beta = 1.8$ and (b) $\tan\beta = 50$. The shaded regions denote the parts of the parameter space (i) producing $\Omega_{\chi_1^0} h^2 < 0.1$ or $\Omega_{\chi_1^0} h^2 > 0.5$, (ii) excluded by theoretical requirements, or (iii) excluded by the chargino search at LEP 2.

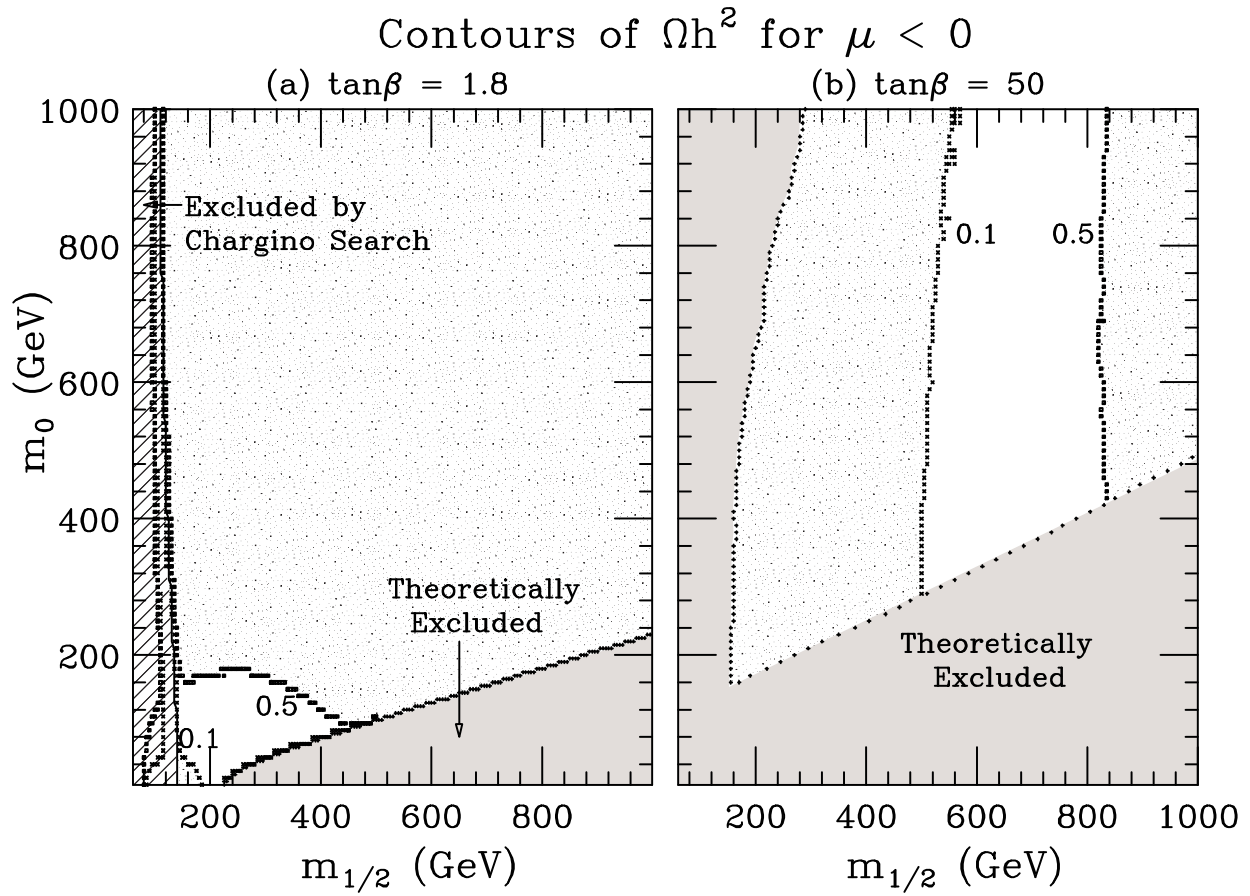


FIG. 8. The same as in Fig. 7, except that $\mu < 0$.

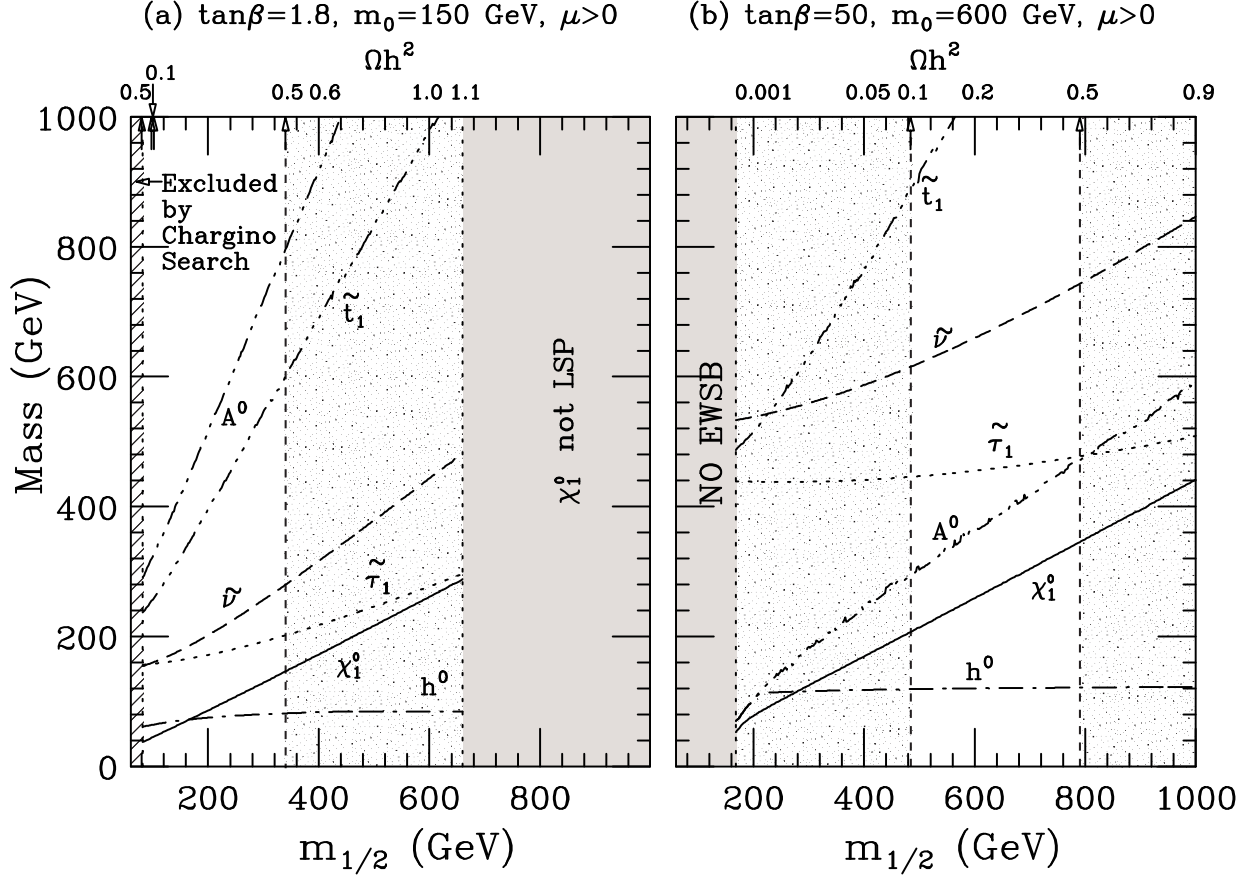


FIG. 9. The neutralino relic density and representative SUSY mass spectrum versus $m_{1/2}$ for $\mu > 0$ with (a) $\tan\beta = 1.8$, $m_0 = 150$ GeV and (b) $\tan\beta = 50$, $m_0 = 600$ GeV. In Figs. 9-12, $\tilde{\nu}$ is the lightest scalar neutrino. The shaded regions denote the parts of the parameter space (i) producing $\Omega_{\chi_1^0} h^2 < 0.1$ or $\Omega_{\chi_1^0} h^2 > 0.5$, (ii) excluded by theoretical requirements, or (iii) excluded by the chargino search at LEP 2.

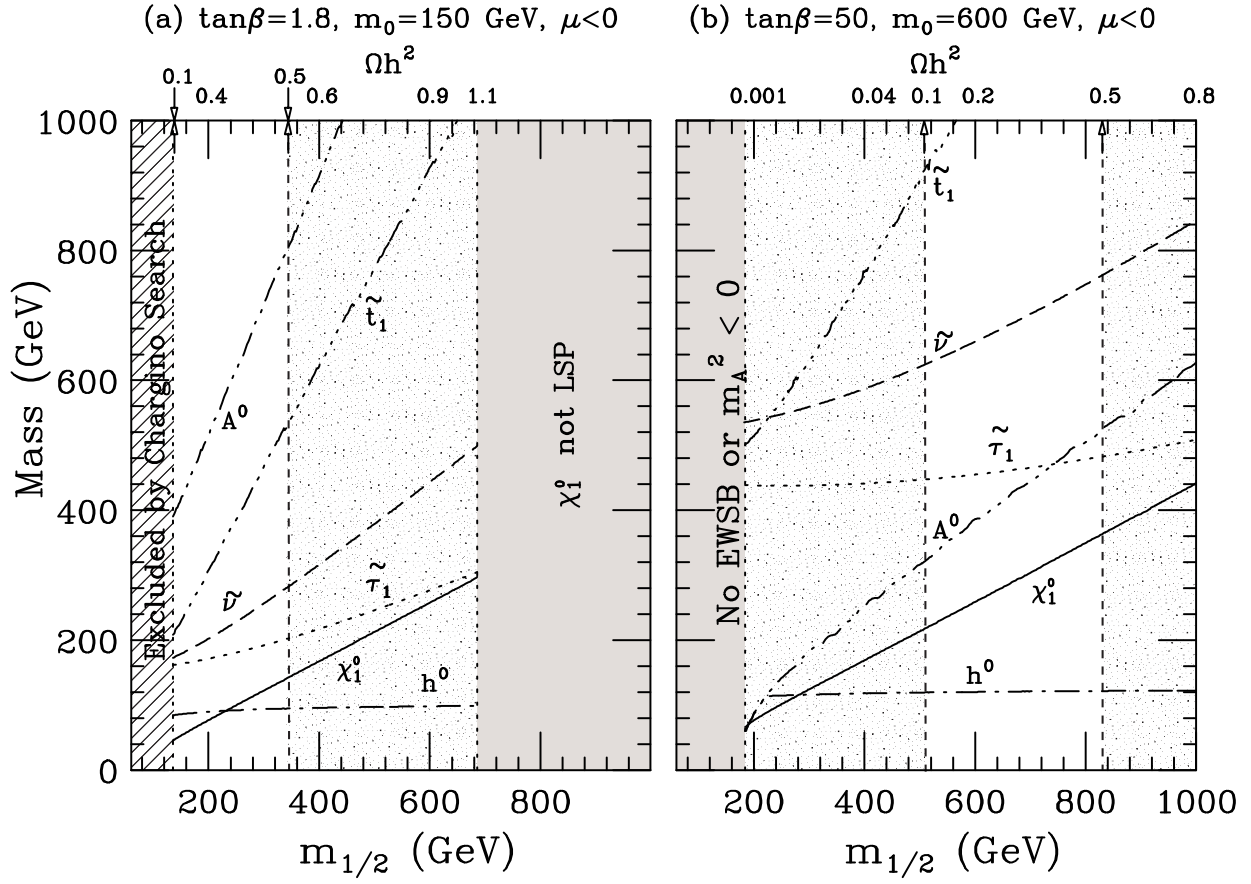


FIG. 10. The same as in Fig. 9, except that $\mu < 0$.

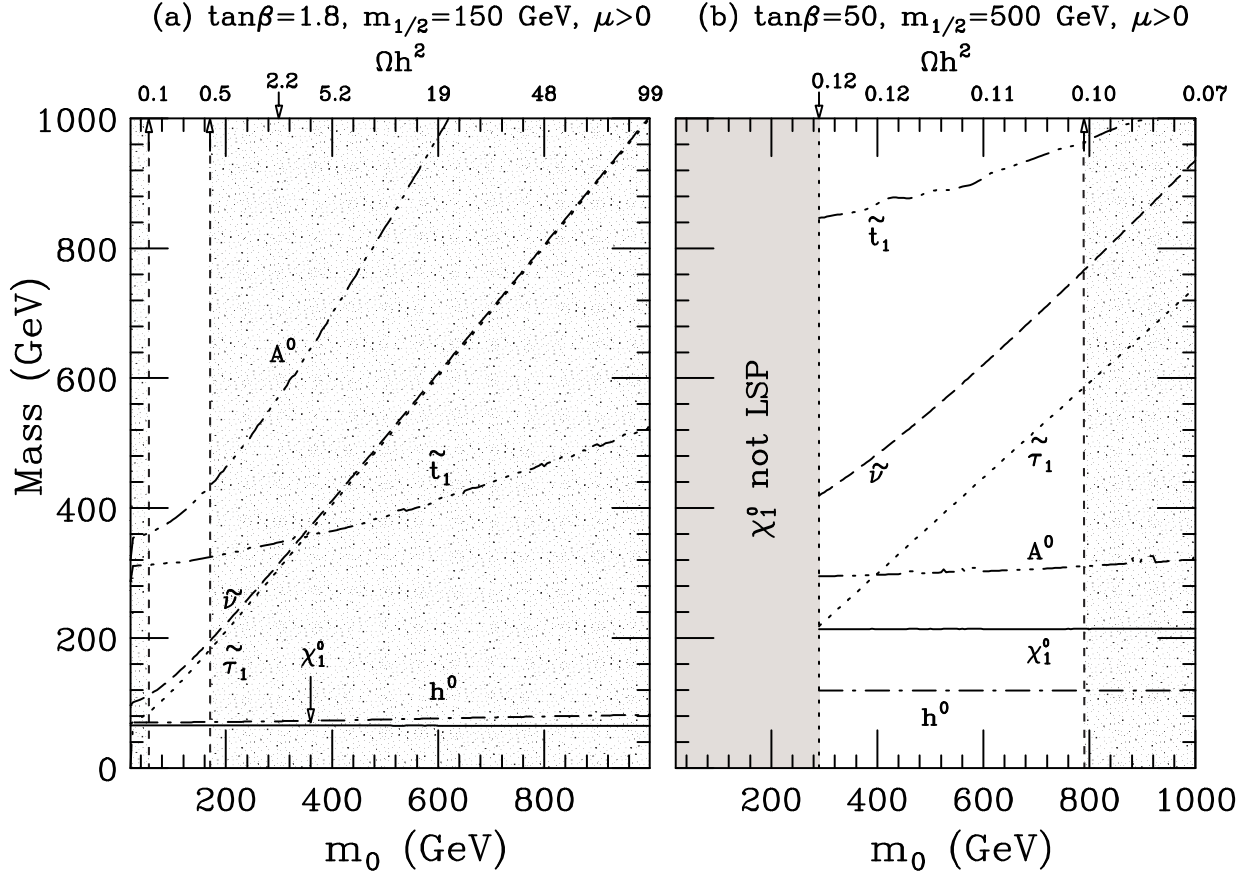


FIG. 11. The neutralino relic density and representative SUSY mass spectrum versus m_0 for $\mu > 0$ with (a) $\tan\beta = 1.8, m_{1/2} = 150 \text{ GeV}$ and (b) $\tan\beta = 50, m_{1/2} = 500 \text{ GeV}$. The shaded regions denote the parts of the parameter space (i) producing $\Omega_{\chi_1^0} h^2 < 0.1$ or $\Omega_{\chi_1^0} h^2 > 0.5$, or (ii) excluded by theoretical requirements.

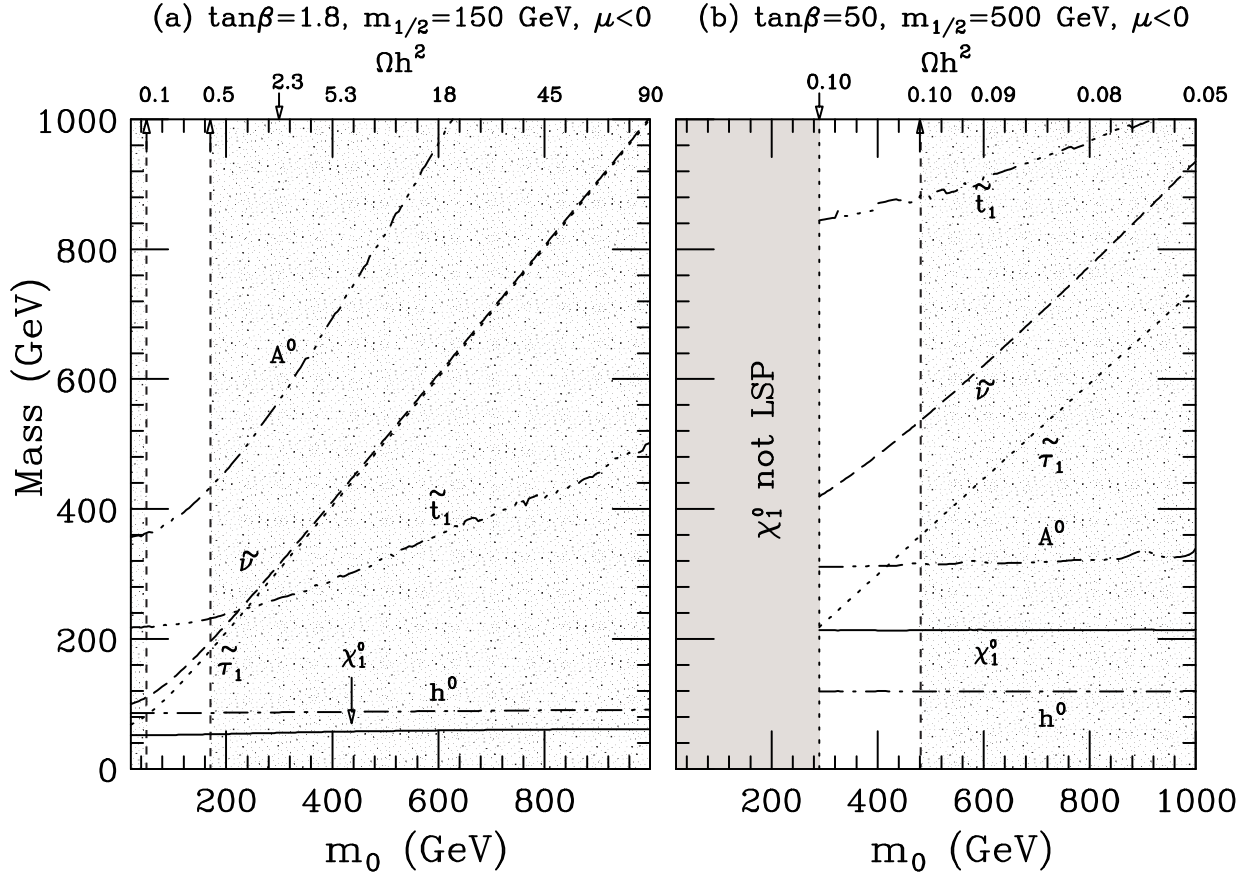


FIG. 12. The same as in Fig. 11, except that $\mu < 0$.

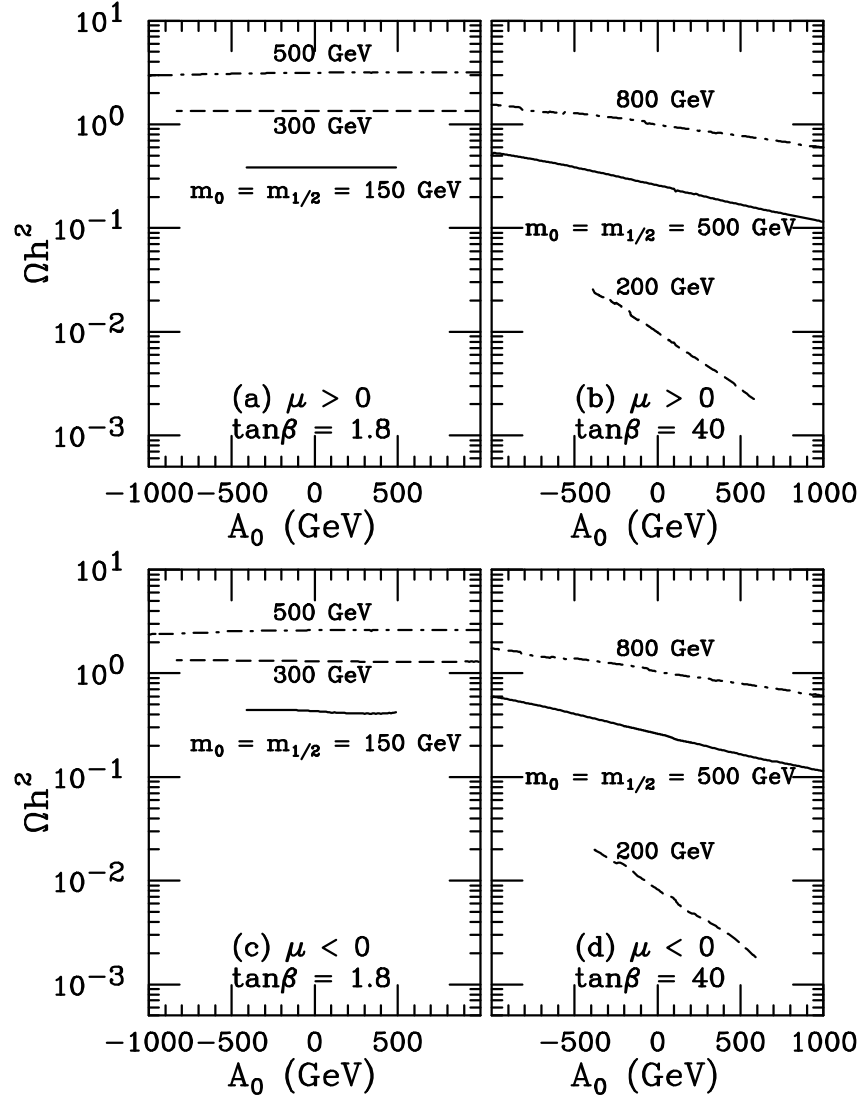


FIG. 13. The neutralino relic density versus the GUT scalar trilinear coupling A_0 for (a) $\mu > 0$ and $\tan\beta = 1.8$, (b) $\mu > 0$ and $\tan\beta = 40$, (c) $\mu < 0$ and $\tan\beta = 1.8$, (d) $\mu < 0$ and $\tan\beta = 40$, and various values of $m_0 = m_{1/2}$.

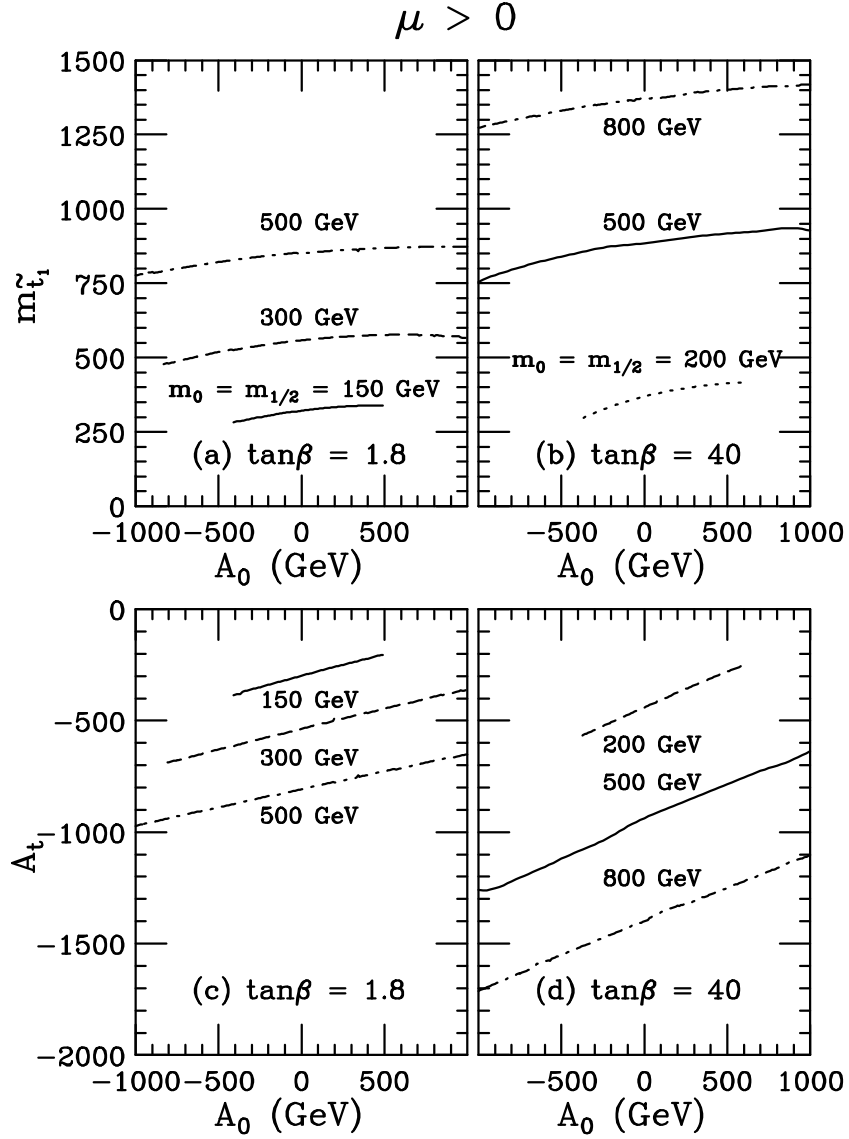


FIG. 14. The mass of the lighter top squark versus A_0 for (a) $\tan\beta = 1.8$, (b) $\tan\beta = 40$, and various values of $m_0 = m_{1/2}$ and $\mu > 0$. Also shown is the soft breaking trilinear coupling A_t at the weak scale versus the GUT scale input A_0 for (c) $\tan\beta = 1.8$, (d) $\tan\beta = 40$,

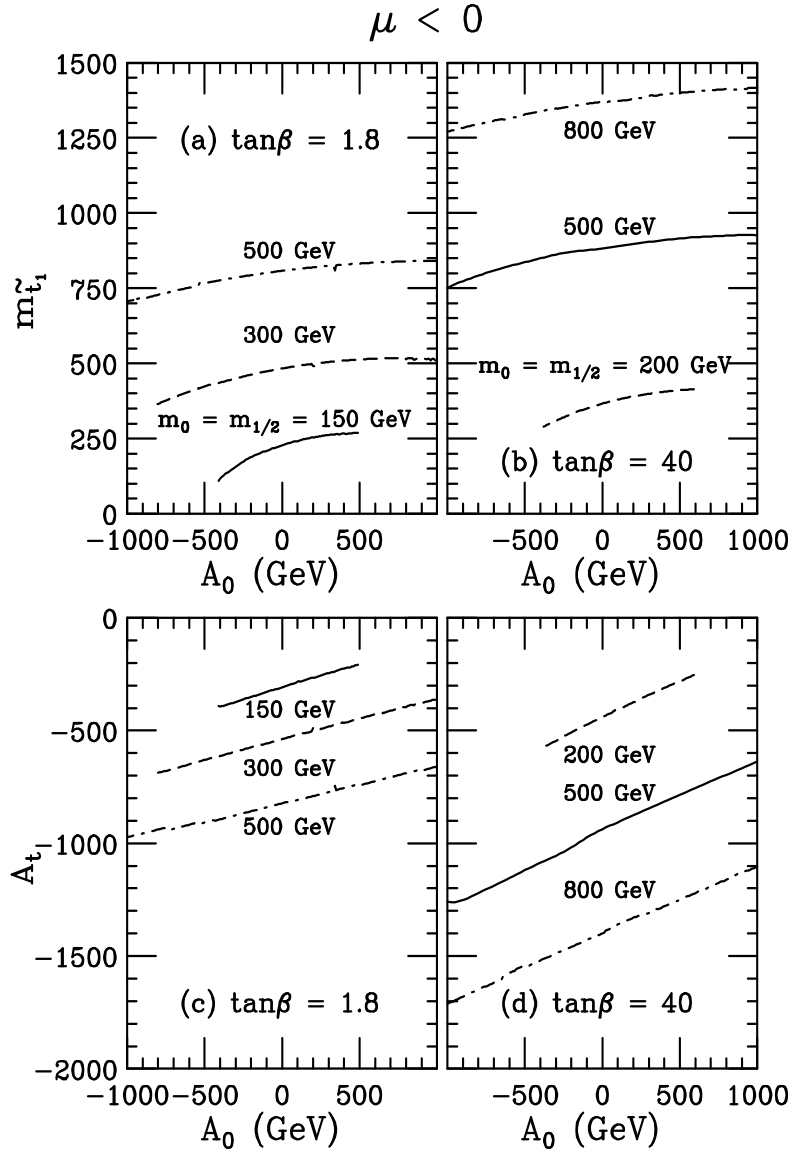


FIG. 15. The same as in Fig. 14, except that $\mu < 0$.